Rock and Soil Mechanics

Volume 41 | Issue 5 Article 6

10-13-2020

Centrifugal shaking table test on dynamic response characteristics of tunnel entrance slope in strong earthquake area

Yang REN

Tian-bin LI
renyang_0616@163.com

Lin LAI

Custom Citation
REN Yang, LI Tian-bin, LAI Lin. Centrifugal shaking table test on dynamic response characteristics of tunnel entrance slope in strong earthquake area[J]. Rock and Soil Mechanics, 2020, 41(5): 1605-1612.

Rock and Soil Mechanics 2020 41(5): 1605−1612
https: //doi.org/10.16285/j.rsm.2019.6161
ISSN 1000−7598
rocksoilmech.researchcommons.org/journal

Centrifugal shaking table test on dynamic response characteristics of tunnel entrance slope in strong earthquake area

REN Yang, LI Tian-bin, LAI Lin

(State Key Laboratory of Geohazard Prevention and Geoenvironment Protection, Chengdu University of Technology, Chengdu, Sichuan 610059, China)

Abstract: The investigation of tunnel damage after strong earthquake shows that the seismic damage of tunnel entrance is quite serious, so it is necessary to further investigate the dynamic response of tunnel entrance slope. Taking the typical tunnel entrance slope in Wenchuan earthquake area as an example, the dynamic response characteristics of tunnel entrance slope under strong earthquake are studied using large centrifugal shaking table test. The experimental results show that: 1) The acceleration amplification on the slope and inside the slope has a significant elevation effect, the acceleration amplification coefficient of the tunnel arch roof is larger than that of the other parts of the tunnel, and the closer to the tunnel entrance the more obvious the acceleration amplification effect. 2) The acceleration amplification effect of the slope is very obvious for different amplitudes, and the acceleration response at low amplitude is larger than that at high amplitude. 3) Under the condition of maintaining 0.25*g* excitation, the acceleration amplification coefficient of slope under different centrifugal load grades is greater than 2.0, but the acceleration magnification factor is basically flat with the increase of centrifugal load. 4) With increasing slope elevation, the dynamic earth pressure decreases linearly, and the dynamic earth pressure response coefficient at the relative elevation of 0.48 (i.e., tunnel arch roof) is the largest. Research results can provide reference for the design and research of seismic mitigation for tunnel entrance in strong earthquake area.

Keywords: tunnel entrance slope; strong earthquake area; centrifugal shaking table test; dynamic response

1 Introduction

With increasing number of tunnels being constructed and increasing frequency of strong earthquake occurrence, tunnels within mountains might be subjected to severe damage. The field investigations after strong earthquakes, such as Kobe earthquake, Chi-Chi earthquake, Wenchuan earthquake, etc., showed that the seismic damage of tunnel entrance is quite severe. The main seismic damages include tunnel entrance slope collapse, entrance rockfall, entrance buried, and tunnel entrance lining cracks, etc.[1–6]. Therefore, the entrance of tunnel is one of the most vulnerable locations under earthquake shaking, and the tunnel entrance slope and the tunnel entrance are the weak parts of tunnels[7]. It is important to further investigate the seismic mitigation for the tunnel entrance slope.

Many scholars have already investigated the dynamic response of tunnel entrance, and most of them utilized the numerical simulations and shaking table model tests, with focuses on the lining structure of tunnel entrance, the influences of seismic mitigation measures and dynamic response[8–17], and relative comprehensive understandings are acquired from these research. However, the results of numerical simulations are different from those of field monitoring, and it is difficult to meet the requirements for reduced-scale model shake table tests due to scaling for gravity. Therefore, scholars have difficulty in capturing the real dynamic response of tunnel entrance slope during earthquake, and especially, there is lack of quantitative analysis.

Nowadays, centrifugal shaking table model test is considered as one of the most advanced methods for investigating the dynamic response and seismic mitigation measures of rock and soil mass[18–19]. The basic procedures are that, the model (1/*n* of the prototype size) is placed in a centrifuge, and the centrifuge is spun to the target gravity state for the model to reach the same stress state as the prototype, and then the scaled earthquake motion can be applied to model. In centrifugal shaking table test, the stress state of the model is consistent with that of the prototype, and the earthquake loading can be accurately reproduced. Most of research utilizing centrifugal shaking table model tests focused on the dynamic response of slope, stability analysis and failure mechanism[20–24], and some scholars conducted this type of test on the seismic response of shield tunnel and seismic mitigation of tunnel[25–26]. However, research on the dynamic response of tunnel entrance slope in the strong earthquake area is rare.

Received: 2 July 2019 Revised: 12 September 2019
This work was supported the Key Program of the State Key Laboratory of Geohazard Prevention and Geoenvironment Protection (SKLGP2011Z002)
First author: REN Yang, male, born in 1984, PhD, Lecturer, mainly engaged in teaching and research on geological engineering and geotechnical engineering. E-mail：renyang_0616@163.com
Corresponding author: LI Tian-bin, male, born in 1964, PhD, Professor, PhD supervisor, mainly engaged in teaching and research on geotechnical engineering and tunnel engineering. E-mail：ltb@cdut.edu.cn

In this paper, a reduced-scale model is built based on the typical characteristics of tunnel entrance slope in Sichuan province, and TLJ-500 centrifugal shaking table in the State Key Laboratory of Geohazard Prevention and Geoenvironment Protection, Chengdu University of Technology, is used to conduct the tests of tunnel entrance slope for further understanding the acceleration and dynamic earth pressure response. The results can provide the scientific basis for the seismic design and mitigation of tunnel entrance in strong earthquake area, and can provide reference for future centrifugal shaking table tests.

2 Centrifugal shaking table model design

2.1 Testing equipment

TLJ-500 centrifugal shaking table system used in this study has two parts, including the centrifuge and the centrifugal shaking table, as shown in Fig. 1. The payload of the centrifuge is 500 $g \cdot$t, and its max acceleration is 250g[22]. The centrifugal shaking table can generate earthquake shaking in horizontal direction with a load capacity of 2t. The max acceleration is 30 g, and the maximum displacement is ±5 mm. The frequency and duration are 20–350 Hz and 5 s, respectively[22].

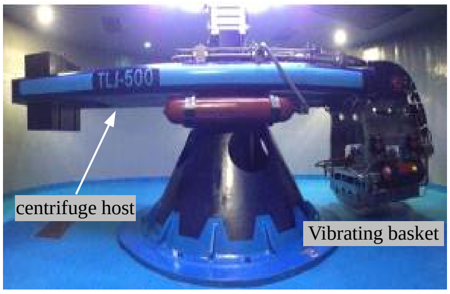

Fig. 1 TLJ-500 centrifuge vibration system

Constraints for the boundaries of the slope are necessary. In order to observe the deformation and failure of slope, a high strength rigid model box with transparent sides and dimensions of 1.0 m (length)× 0.6 m (width)×0.7 m (height) is selected (Fig. 2).

Fig. 2 Rigid model box

2.2 Similitude relationship

Considering the capacity of the centrifugal shaking table system, combined with the purpose of this centrifuge model test and factors such as the size and spatial location of the tunnel model, the maximum centrifugal acceleration of this test is preset to 50g, and the scale of the model to the prototype is N=1:50.. Main similitude ratios of the tests are shown is Table 1.

2.3 Model design and material selection

Based on the typical characteristics of tunnel entrance slope (Yingxiu tunnel, Taoguan tunnel, etc.) in the strong earthquake area of Sichuan province, the model is simplified but holds on main features of the prototype, as shown in Fig.3. Main features and dimensions are introduced as follows.[27] The model just has one smooth slope with no topographic relief, and the slope ratio is 1:1.25. Length, width, and height of the model are 100 cm, 60cm and 65cm, respectively. The thickness of model foundation is 15 cm, and the height of model slope is 50 cm. The tunnel with 12 cm diameter is located in the lower half of model slope. The distance between the bottom of tunnel and the toe of the slope is 12 cm in the vertical direction. The distance between the top of the tunnel and the top of the slope is 26 cm. The axial direction of the tunnel is the same as the direction of the slope.

Table 1 Similarity scale of main physical quantity in centrifugal vibration test

Physical quantity	Formula	Similarity scale
Density ρ	C_ρ	1
Cohesion c	$C_c = C_E$	1
Internal fraction angel φ	C_φ	1
Strain ε	$C_\varepsilon = C_\rho C_a C_l C_E^{-1}$	1
Length l	$C_l = C_\varepsilon C_E / C_\rho C_a$	1/50
Shaking frequency f	$C_f = C_t^{-1}$	50
Displacement u	$C_u = C_l C_\varepsilon$	1/50
Shaking acceleration a	$C_a = C_u C_t^{-2}$	50
Gravity g	C_g	50

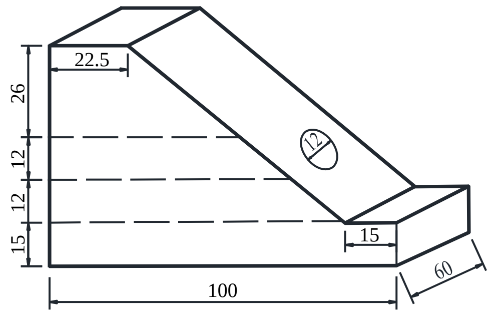

Fig. 3 Centrifugal model and dimension (unit：cm)

The soil of tunnel entrance slope belongs to the quaternary overburden layer. According to the feather and composition of the soils, considering the similarity scale in Table 1, the scale factors of density, cohesion and internal friction angle are 1. The soil was prepared based on the physical and mechanical properties of field soil. Considering the particle size of soil, the physical and mechanical parameters of soil used in the model tests were the same as the field soil. For the field soil, water content is 12%, density is 2.5 g/cm^3, cohesion c is 21 kPa, and internal friction angle φ is 27°. After several trial preparations, particle size composition and their percentage are listed in Table 2.

Table 2 Particle size composition of soil mass

Grain size/ mm	0.047	0.074	0.2	0.25	0.5	1	2
Percentage/ %	15	10	15	25	25	5	5

This study focuses on the dynamic response of tunnel entrance slope, so the tunnel model could be simplified and made by high strength material. Through many trial tests, polymethyl methacrylate (PMMA) is chosen as the material for the tunnel model. The section of the tunnel model is round at one end and ellipse at the other end. Length, external diameter, and thickness of the tube are 70 cm, 12 cm and 1cm, respectively, and the PMMA tunnel model is present in Fig. 4.

Fig. 4 Tunnel model

2.4 Sensor layout

Instrumentation for the model included 10 accelerometers, 4 dynamic earth pressure cells and 2 static earth pressure cells, and 1 displacement sensor. The accelerometer A1 (A1 for short) was fixed on the bottom outside the model box. A2 was placed at the slope toe; A4 and js1 were symmetrically arranged based on the longitudinal center plane of the model; A3, A5, A8 and A9 were placed near the earth pressure cells; A7 and A10 were embedded in the inner side of the slope at the same elevation as A5 and A9, respectively; and A5, A6 and A7 were at the same elevation, and A6 was located between A5 and A7. The distance between A6 and A5 was the same as that between A6 and A7. Four dynamic earth pressure cells, ds1, ds2, ds3 and ds4, were placed within slope from the bottom up.The locations of all sensors installed inside model slope are illustrated in Figs.5 (a) and 5(b).

2.5 Model construction

Model construction included: (i) Vaseline was smeared on the inside wall of the model box, and the 15 mm plastic boards manufactured with elastic particle were placed in the model box for reduction of friction and waves reflection. (ii) The grid paper with the slope outlined was pasted on the two sides of the model box. The prepared soil was paved and compacted in layers, and the tunnel model and sensors were placed at the designed location. (iii)The slope was made smooth and then covered by plastic membrane to prevent evaporation. The prepared model is shown in Fig. 6.

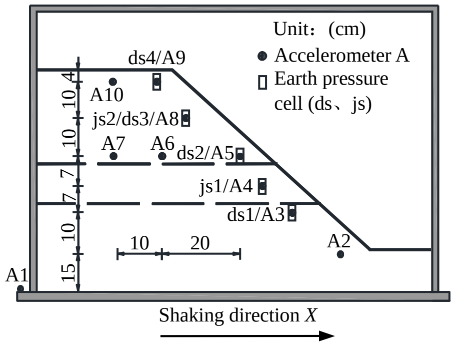

(a) Side view of sensors layout

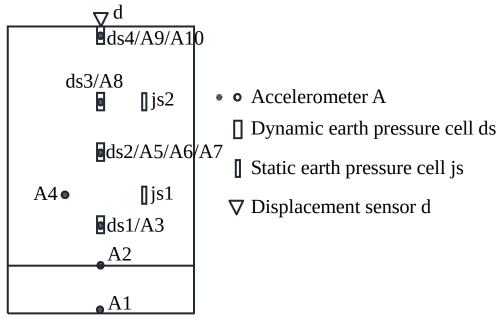

(b) Front view of sensors layout

Fig. 5 Sensor layout diagram

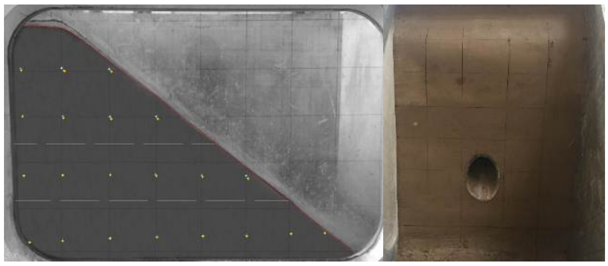

Fig.6 Side and front photos of model

2.6 Earthquake motion input and loading scheme

This test focuses on the dynamic response of tunnel entrance slope under Wenchuan earthquake. The earthquake motion recorded by the Wolongtai station was used, and the time-history of horizontal acceleration can be seen in Fig.7. Recorded Wenchuan earthquake accelerations were scaled first, and then applied in the test.

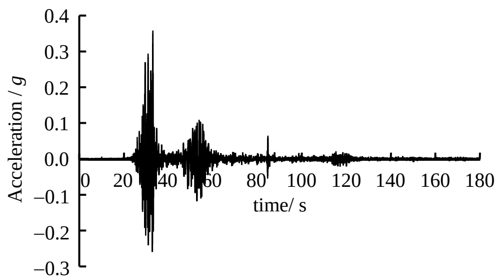

Fig. 7 Time-history of horizontal acceleration

The multi-stage loading was used in this study. The model was subjected to shaking in the direction of the slope with a dominant frequency of 270Hz. Loading sequences were as follows. (a) Four accelerations, 30*g*, 50*g*, 60*g* and 70*g* were loaded to the model successively. According to the similarity ratio *N*=1:50, shaking table tests were conducted under different accelerations, with the focus on 50*g*. For acquiring the dynamic response of slope under various centrifugal accelerations and earthquake excitation, the shaking table tests under different centrifugal accelerations such as 30*g*, 60*g* and 70*g* were also conducted. In addition, the peak earthquake acceleration of 0.3*g* was adopted to scale accelerations based on the recorded Wenchuan earthquake motion. So, the tests under higher centrifugal acceleration and vibration acceleration were not conducted. (b) Shaking was applied to the model after the centrifugal acceleration reached to the target value and the earth pressure remained stable. (c) When the shaking step finished, the centrifuge should run approximately 50s. The next loading did not start until the earth pressure was stable. The shaking plan is shown in Table 3.

Table 3 Summary of various loading schemes

Testing condition	Centrifugal acceleration / *g*	Shaking acceleration / *g*	Prototype earthquake acceleration / *g*
Testing condition 1	30	4.5	0.15
Testing condition 2	50	7.5	0.15
Testing condition 3	50	12.5	0.25
Testing condition 4	50	15.0	0.30
Testing condition 5	60	15.0	0.25
Testing condition 6	70	17.5	0.25

3 Seismic response of tunnel entrance slope

For the convenience of analyzing the dynamic response of tunnel entrance slope, such as acceleration, earth pressure, etc., some definitions are made as follows[27]:

(1) Acceleration amplification coefficient *R*: the ratio of the peak acceleration at any point in the slope to the peak acceleration of shaking table. Table 4 gives the values of *R* under different testing conditions.

(2) Dynamic earth pressure response coefficient: the ratio of the difference between the maximum value and the minimum value of measured dynamic earth pressure to the initial value of dynamic earth pressure.

(3) Relative horizontal distance (d/D): the ratio of the distance between the acceleration sensor and the rear wall of the model box to the total length of model at certain height.

(4) Relative elevation (h/H): the ratio of the vertical distance between the acceleration sensor and the toe of the slope to the vertical distance between the top of the slope and the toe of the slope.

The acceleration amplification coefficient *R* (PHA) of each measuring point is greater than 1.0 (Table 4) , which has obvious amplification effect under different testing conditions. However, the extent of amplification effect at different locations is different. The most obvious amplification effect appears at the tunnel arch roof (A5). The dynamic response characteristics are analyzed through correlation curves about the mean values of *R* under various conditions.

Table 4 Acceleration amplification coefficient *R* under different test conditions

Testing conditions	acceleration amplification coefficient *R* of different monitored points								Mean value
	A3	A4	A5	A6	A7	A8	A9	A10	
Testing condition 1	1.45	1.71	1.81	1.37	1.17	1.98	2.82	2.55	1.86
Testing condition 2	1.69	2.48	2.75	2.50	2.05	3.17	3.62	2.50	2.60
Testing condition 3	1.50	1.64	2.58	1.98	1.53	2.72	3.20	2.66	2.23
Testing condition 4	1.34	1.41	2.49	2.00	1.43	2.26	2.45	2.35	1.97
Testing condition 5	1.45	1.40	2.95	1.75	1.36	2.66	2.92	2.32	2.10
Testing condition 6	1.38	1.24	2.72	1.76	1.17	2.56	2.97	2.52	2.04
Mean value	1.47	1.65	2.55	1.89	1.45	2.56	2.99	2.48	—

3.1 Horizontal acceleration on the slope surface

The relationships of acceleration amplification coefficient *R* versus relative elevation (h/H) of five monitored points (A3, A4, A5, A8, A9) are plotted in Fig. 8. Acceleration amplification coefficient *R* increases with increasing relative elevation. At the points of relative elevation 0.36, 0.48, 0.68 and 0.88, the values of *R* increase by 0.18, 0.90, 0.01 and 0.43, compared to the previous point, respectively. The increase trend is not linear. At the point of $h/H = 0.48$, the value of *R* increases by 0.90 and reaches 2.55. It can be concluded that the horizontal acceleration amplification effect of slope is influenced by both the height and the tunnel within slope. Acceleration amplification coefficient *R* increases with increasing elevation, which shows the obvious elevation effect that is consistent with the dynamic response of slope without tunnel[22]. Because the tunnel arch roof has higher elevation and is closer to the top of the slope, the acceleration amplification effect of this position is more conspicuous. In addition, the existence of tunnel in the lower half slope leaves larger free face in that location and more slope deformation, leading to a sharp increase of acceleration amplification coefficient, which is consistent with findings from previous studies[28]. In short, during the earthquake, the existence of tunnel cause remarkable free face point effect and height effect on the amplification of acceleration. The acceleration amplification coefficient *R* has a sharp increase at the tunnel arch roof, which would cause a negative influence on the safety of lining of tunnel arch roof and structure. This is consistent with the fact that earthquake damage is more severe at the tunnel arch roof, as discovered in earthquake investigations.

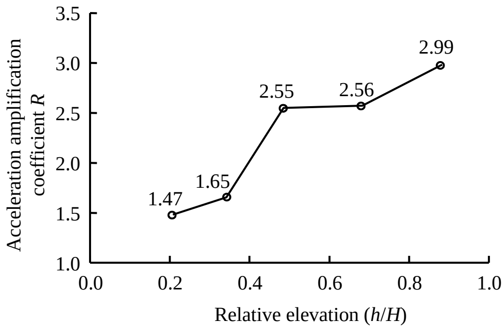

Fig. 8 *R* values of slope surface at different elevations

3.2 Horizontal acceleration inside the slope

The relationship curves between relative elevation (h/H) and acceleration amplification coefficient *R* of four monitored points (A6, A7, A9 and A10) inside the slope are depicted in Fig. 9. Inside the slope, *R* values are increase with the relative elevation increasing at the same vertical line. The relative elevations of four monitored points are between 0.48 and 0.88. Acceleration amplification coefficients of A6 and A7, at lower elevations, are 1.45 and 1.89, respectively, while those of A9 and A10, at higher elevations, are 2.48 and 2.99, respectively. *R* values of A9 and A10, which close to the top of the slope (higher elevation), increase by 0.44 and 0.41 compared to those of A6 and A7, inside the slope with lower elevations. Thus, inside the slope, the more close to the top of the slope, the more significant acceleration amplification effects, and there is an evident height effect on *R* values.

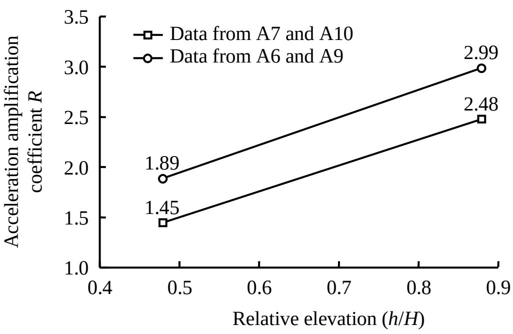

Fig. 9 *R* values inside slope at different elevations

Figure 10 gives the relationship curves between relative horizontal distance (d/D) and acceleration amplification coefficient *R* of five monitored points (A5, A6, A7, A9 and A10) inside the slope.

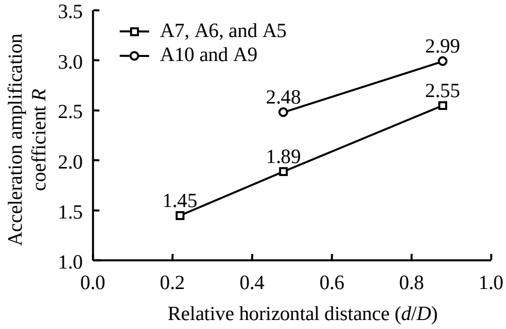

Fig. 10 *R* values inside slope at different relative horizontal distances

At the same elevation, *R* values approximately increase with the increasing of relative horizontal distance, and acceleration amplification effects are more prominent with decreasing distance between the monitored point and the slope surface. When the relative horizontal distance is between 0.22 and 0.88, *R* values of A7, A6 and A5, at the top of the tunnel, are 1.45, 1.89 and 2.55, respectively, while *R* values of A10 and A9, at the top of the slope, are 2.48 and 2.99, respectively. Acceleration amplification effects of A5 and A9 which close to the slope surface are most notable. Thus, acceleration amplification effects are more evident with relative horizontal distance increaseing and with closer to the slope surface, and these effects at A5 which is at the tunnel arch roof and close to the slope surface are quite obvious. So, earthquake damages such as landslide and collapse are easy to occur at the entrance of tunnels.

3.3 Slope acceleration response under different excitation amplitudes

For further investigating slope acceleration response under different amplitudes, shaking table tests under three prototype motion with amplitudes of 0.15*g*, 0.25*g* and 0.30*g*, were conducted with 50*g* centrifugal loading. Results show that acceleration response under earthquake shaking on the slope and inside the slope are similar. For convenience, the mean values of acceleration amplification coefficient at all monitored points are used to analyze the dynamic response. Figure 11 presents the variation of average values of *R* with the amplitude of earthquake.

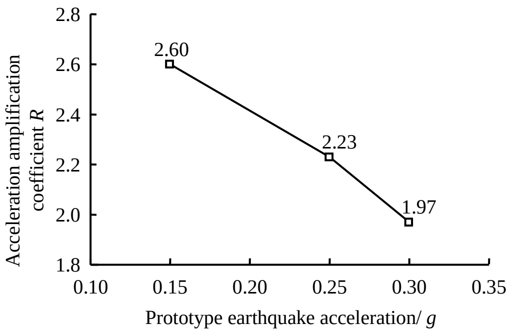

Fig. 11 Means of *R* under different excitation amplitudes

As shown in Fig.11, R values of tunnel entrance slope under amplitudes of 0.15g, 0.25g and 0.3g, are 2.60, 2.23 and 1.97, respectively, exhibiting an obvious amplification effect. R values decrease almost linearly with increasing amplitude, and the acceleration amplification coefficients for small amplitudes are larger than for larger amplitudes, implying acceleration amplification effects for small amplitudes are more evident.

3.4 Slope acceleration response under different centrifugal accelerations

The study not only involved shaking table tests under the centrifugal acceleration decided by the similarity ratio, N=1:50, but also the shaking table tests under multi-stage centrifugal accelerations such as 50g, 60g and 70g. These tests under different centrifugal accelerations have the same peak earthquake acceleration of 0.25 g, and the results can be used to analyze the dynamic response of tunnel entrance slope under different centrifugal accelerations.

Acceleration amplification coefficients of different centrifugal accelerations are shown in Fig.12. Dynamic response of slope with 0.25 g peak acceleration is very strong under various centrifugal accelerations, and all the means of acceleration amplification coefficient R of all monitored points exceed 2. However, the means of R decrease with increasing centrifugal acceleration. In addition, the means of R under higher centrifugal accelerations are slightly smaller than those under lower centrifugal accelerations. Thus, the increase of centrifugal accelerations has a relatively small influence on acceleration amplification effects of slope.

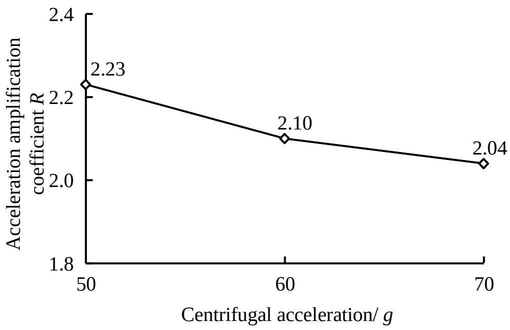

Fig. 12 Means of *R* under different centrifugal conditions

3.5 Dynamic earth pressure response

Four dynamic earth pressure sensors were buried inside the slope of the models. ds4 (with a relative elevation of 0.88) at the top of the slope was damaged in the tests. This paper includes analysis of the maximum dynamic earth pressure and response for three other dynamic earth pressure sensors (ds1, ds2 and ds3). The maximum values of dynamic earth pressure of monitored points are depicted in Fig. 13, and the dynamic earth pressure response coefficients are shown in Fig. 14.

Figure 13 shows that, with the relative elevation of monitored points increasing from ds1 to ds2 and then to ds3, the maximum values of dynamic earth pressure decrease from 21.35 kPa to 6.53 kPa. The difference between adjacent points are 8.10 kPa and 6.72 kPa, respectively. Dynamic earth pressure of slope decreases linearly with increasing elevation.

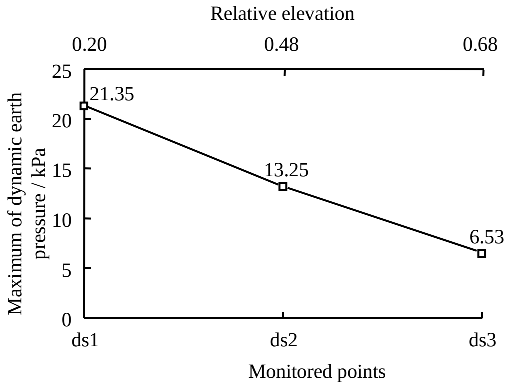

Fig. 13 Maximum dynamic earth pressures at different elevations

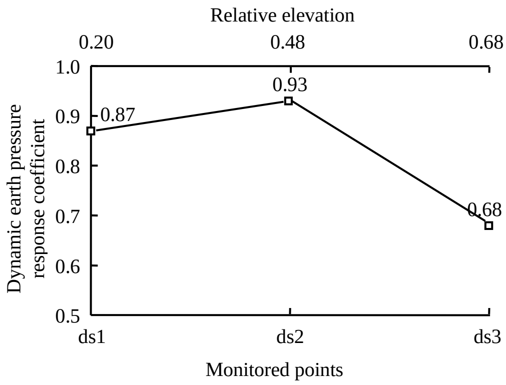

Fig. 14 Dynamic earth pressure response coefficients at different elevations

Relative elevations of three monitored points, ds1, ds2 and ds3, are 0.2, 0.48 and 0.68, respectively, and ds2 is at the tunnel arch roof. As shown in Fig.14, dynamic earth pressure response coefficients are 0.87, 0.93 and 0.68. Thus, there is a linear relationship between the magnitude of dynamic earth pressure inside the slope and the elevation, and higher dynamic earth pressure would occur at deeper location (lower elevation). In addition, according to the ratio of the increment of dynamic earth pressure to the value of initial dynamic earth pressure, i.e., dynamic earth pressure coefficient, dynamic earth pressure response near the tunnel is more intense, which is mainly because of the existence of the tunnel. This is similar to the acceleration response on the slope. It is concluded that, the intense dynamic earth pressure response in the vicinity of the tunnel has an adverse effect on the safety of tunnel structure, especially the lining of the tunnel arch roof.

4 Conclusions

This paper choses the typical tunnel entrance slope of Wenchuan earthquake-stricken area as the prototype of centrifugal shaking table tests to investigate the dynamic response characteristics of tunnel entrance slope under strong earthquake. Conclusions are as follows:

(1) The acceleration amplification effect of tunnel entrance slope under strong earthquake increases linearly. Not only the elevation effect, but the existence of tunnels has an evident influence on the acceleration amplification coefficients. There is a sharp increase on the tunnel arch roof for acceleration amplifications. The closer to tunnel entrance, the more obvious the acceleration amplification effect is. It is observed that, on the tunnel arch roof, the superpose- tion effect of free face points effect and elevation effect is evident for acceleration amplification. Thus, tunnel entrance and the tunnel arch roof would suffer more severe earthquake damage under a strong earth- quake.

(2) With the same centrifugal acceleration of 50*g*, the acceleration amplification coefficients (R) of the slope exceed 1.5 under earthquake excitations with different amplitudes of 0.15 *g*, 0.25 *g* and 0.3 *g*. Acceleration amplification effect is considerably obvious under earthquake motions with different acceleration amplitudes, and the acceleration response is stronger under lower amplitudes whereas smaller under higher amplitudes.

(3) Under the earthquake shaking with acceleration of 0.25 *g*, acceleration amplification effect of the slope is very obvious under the centrifugal loading of 50 *g*, 60 *g* and 70 *g*. The means of amplification coefficients all exceed 2.0, but the influence of centrifugal loading on amplification effect is small. The differences of acceleration amplification coefficients under different centrifugal loadings are also small.

(4) Dynamic earth pressure decreases linearly with increasing elevation. Although amplification effect is not evident, dynamic earth pressure on the tunnel arch roof (relative elevation of 0.48) is more intense than the other locations, which might cause an adverse effect on the lining safety of the tunnel arch roof.

It is found from post-earthquake investigations that tunnel entrance is one of parts that suffers most severe seismic damage, and therefore the dynamic response of tunnel entrance slope draws attention from geological and geotechnical engineering. In fact, some other factors, such as slope structure, material composition and earthquake characteristics, also have influences on the dynamic response. This study chose the typical tunnel entrance slope as the prototype, and construct the model by simplifying the prototype. The universality and the representativeness of the model are insufficient, and more verification and supplement are needed in future study.

References

[1] LI Tian-bin. Failure characteristics and influence factor analysis of mountain tunnels at epicenter zones of great Wenchuan earthquake[J]. Journal of Engineering Geology, 2008, 16(6): 742–750.

[2] WANG W L, WANG T T, SU J J, et al. Assessment of damage in mountain tunnels due to the Taiwan Chi-Chi earthquake[J]. Tunnelling and Underground Space Technology, 2001, 16(3): 133–150.

[3] GAO Bo, WANG Zheng-zheng, YUAN Song, et al. Lessons learnt from damage of highway tunnels in Wenchuan earthquake[J]. Journal of Southwest Jiaotong University, 2009, 44(3): 336–341.

[4] WANG Z Z, GAO B, JIANG Y J, et al. Investigation and assessment on mountain tunnels and geotechnical damage after the Wenchuan earthquake[J]. Science in China (Series E: Technological Sciences), 2009(2): 546–558.

[5] CUI Guang-yao, WU Xiu-gang, WANG Ming-nian, et al. Earthquake damages and characteristics of highway tunnels in the 8.0-magnitude Wenchuan earthquake[J]. Modern Tunnelling Technology, 2017(2): 9–16.

[6] CHEN Z Y, CHENG S, LI T B. Damage characteristics and influence factors of mountain tunnels under strong earthquakes[J]. Natural Hazards, 2012, 61(2): 387–401.

[7] DOWDING C H, ROZEN A. Damage to rock tunnels from earthquake shaking[J]. Journal of the Geo- technical Engineering Division, 1978, 10(4): 175–191.

[8] CUI Guang-yao, JI Lei, WANG Ming-nian, et al. Shock absorber with rigid-flexible combination model tests for tunnel opening section in high intensity seismic areas[J]. Journal of Vibration and Shock, 2019, 38(5): 92–97.

[9] JIANG Shu-ping, WEN Dong-liang, ZHENG Sheng-bao. Large scale shaking table test for seismic response in portal section of Galongla tunnel[J]. Chinese Journal of Rock Mechanics and Engineering, 2011, 30(4): 649–657.

[10] YE Hai-lin, ZHENG Ying-ren, DU Xiu-li, et al. Shaking table model test and numerical analysis on dynamic failure characteristics of slope[J]. China Civil Engineering Journal, 2012, 45(9): 128–135.

[11] WANG Shuai-shuai, GAO Bo, SUI Chuan-yi, et al. Shaking table test for seismic behavior of upward slope at tunnel entrance in different geological conditions[J]. Rock and Soil Mechanics, 2014, 35(Suppl.1): 278–285.

[12] WU Dong, GAO Bo, SHEN Yu-sheng, et al. Shaking table test study of seismic dynamic response of tunnel entrance slope[J]. Rock and Soil Mechanics, 2014, 35(7): 1921–1929.

[13] TAO Lian-jin, HOU Sen, ZHAO Xu, et al. Large-scale

shaking table test for dynamic response in portal section of mountain tunnel with different gradients of upward slope[J]. Rock and Soil Mechanics, 2014, 35(Suppl.1): 92–97.

[14] CAO Jun. Experimental study with vibrating table on dynamic response characteristics of side slopes at tunnel portals[J]. Technology of Highway and Transport, 2015(3): 85–89.

[15] HOU Sen, TAO Lian-jin, ZHAO Xu. Dynamic response of portal section of mountain tunnels under seismic SH wave action[J]. Chinese Journal of Rock Mechanics and Engineering, 2015, 34(2): 340–348.

[16] GUAN Z C, ZHOU Y, GOU X D, et al. The seismic responses and seismic properties of large section mountain tunnel based on shaking table tests[J]. Tunnelling and Underground Space Technology, 2019, 90: 383–393.

[17] XIN C L, WANG Z Z, ZHOU J M, et al. Shaking table tests on seismic behavior of polypropylene fiber reinforced concrete tunnel lining[J]. Tunnelling and Underground Space Technology, 2019, 88: 1–15.

[18] YU Yu-zhen, DENG Li-jun, LI Rong-jian. Centrifuge model test of the seismic response behavior of a sand slope[J]. Journal of Tsinghua University (Science and Technology), 2007, 47(6): 789–792.

[19] TABOADA V M, MARTINEZ-RAMIREZ G, ABDOUM T. Centrifuge modeling of seismic behavior of a slope in liquefiable soil[J]. Soil Dynamics and Earthquake Engineering, 2002, 22(9): 1043–1049.

[20] YU Y, DENG L, SUN X, et al. Centrifuge modeling of a dry sandy slope response to earthquake loading[J]. Bulletin of Earthquake Engineering, 2008, 6(3): 447–461.

[21] TU Jie-wen, LIU Hong-shuai, TANG Ai-ping, et al. Acceleration response of colluvial landslide based on centrifugal shaking table test[J]. Chinese Journal of Rock Mechanics and Engineering, 2015, 34(7): 1361–1369.

[22] JU Neng-pan, DENG Tian-xin, LI Long-qi, et al. Centrifugal shaking table test on toppling deformation mechanism of steep bedding slope under strong earthquake[J]. Rock and Soil Mechanics, 2019, 40(1): 99–109.

[23] YU Y Z, DENG L J, SUN X, et al. Centrifuge modeling of a dry sandy slope response to earthquake loading[J]. Bulletin of Earthquake Engineering, 2008, 6(3): 447–461.

[24] WANG L P, ZHANG G. Centrifuge model test study on pile reinforcement behavior of cohesive soil slopes under earthquake conditions[J]. Landslides, 2014, 11(2): 213–223.

[25] HUANG Mao-song, CAO Jie. Simplified analysis of tunnel earthquake response and centrifuge modelling calibration[J]. Chinese Journal of Rock Mechanics and Engineering, 2010, 29(2): 271–280.

[26] CHEN Z Y, SHEN H. Dynamic centrifuge tests on isolation mechanism of tunnels subjected to seismic shaking[J]. Tunnelling and Underground Space Technology, 2014, 42: 67–77.

[27] LAI Lin. Centrifugal model test study of entrance slope under earthquake[D]. Chengdu: Chengdu University of Technology, 2016.

[28] BIAN Lei, LIANG Qing-guo, ZHANG Qin-peng. Experimental study on seismic responses of slope and portal of loess tunnel[J]. Railway Standard Design, 2018, 62(3): 79–85.